Journal of Heat and Mass Transfer Research

Journal homepage: https://jhmtr.semnan.ac.ir

Semnan University

ISSN: 2383-3068

Research Article

Evaluation of Mass Transfer Characteristics of Reverse Osmosis Desalination Process Based on the Spiegler-Kedem-Katchalsky Model

Dnya Sharif Mohammed [a]*, Ibtisam Kamal [b], Abdulsamad Abdulhameed [c]

[a] *Kurdistantechnical Institute, Kurdistan Region, Iraq*

[b] *Petroleum Engineering Department, College of Science and Technology, University of Basrah, Basrah, Iraq*

[c] *Siemens Energy, Department of Operation, Khormala Power Plant, Erbil, Iraq*

ARTICLE INFO

Article history:

Received: 2024-03-14

Revised: 2025-08-16

Accepted: 2025-08-24

Keywords:

Mass transfer coefficient;

Temperature;

Recovery;

Water permeability;

Salt permeability;

Permeate flux.

ABSTRACT

In previous work, the reverse osmosis (RO) process was evaluated based on the potential synergy of Process Design and response surface methodology (RSM) methodologies, and the effects of membrane age, percentage recovery, concentrations of salts, pH, temperature, and pressure of feed water and the rejected brine concentration were optimized and modeled. The current work includes the determination of phenomenological parameters of mass transfer for RO membrane systems using the Spiegler-Kedem-Katchalsky model. The mass transfer coefficient and membrane permeability for salts were determined as a function of temperature and percentage recovery. The calculations of mass transfer parameters were based on a reference RO membrane (ESPA4-LD-4040), a three stage RO process, a 3-year membrane age with 95% and 85% recovery, a permeate flow 20 m^3/h, pH 7, a constant feed TDS of 800 mg/l, constant pump pressure for feed water of 15 bar, and feed-water temperatures of 4, 8.2, 25, 30, and 42^oC. The results showed that when the temperature increases from 4°C to 42^oC, the mass transfer coefficient increases by 35.44% for 95% recovery, and 83.97% for 85% recovery, respectively. A general mathematical model describing the relationship between the mass transfer coefficient and feed water temperature, water permeability, and salt permeability was developed. The Spiegler-Kedem-Katchalsky model proved its capability for membrane performance evaluation through the determination and correlation of the phenomenological parameters of mass transfer for the membrane system.

1. Introduction

The future looming shortage of drinking water demands urgent intervention. Addressing this issue, the desalination of seawater and brackish water emerges as a viable alternative. The primary techniques employed for demineralizing water with an excess of salts are nanofiltration and reverse osmosis [1]. However, this approach introduces complexity in terms of mass transfer mechanisms, involving (i) convection, driven by the pressure gradient Δp, and (ii) diffusion, occurring due to the concentration gradient. Different methods have been utilized in the literature to describe RO membrane parameters and the mass transfer

* **Corresponding author.**

E-mail address: mohammadi@gmail.com

Cite this article as:

Mohammed, D.S., Kamal, I., and Abdulhameed, A., 2026. Evaluation of Mass Transfer Characteristics of Reverse Osmosis Desalination Process Based on the Spiegler-Kedem-Katchalsky Model. *Journal of Heat and Mass Transfer Research*, 13(4), pp. 439-447.

https://doi.org/10.22075/JHMTR.2025.33417.1527

coefficient (k). These methods include (a) direct measurements, employing optical or microelectrode techniques; (b) indirect measurements, where the true rejection is determined through extrapolation to infinite feed circulation; and (c) indirect measurements, where the mass transfer coefficient is calculated using a concentration polarization model combined with a membrane transport model. Nevertheless, each of these approaches comes with its own set of advantages and disadvantages [2]. Current recognition supports the use of a three-parameter model, such as the Spiegler-Kedem model. The SKK model uses three parameters to characterize transport: the reflection coefficient, solute permeability, and water permeability. Calculation of the concentration at the membrane surface is required to estimate reflection coefficient and solute permeability; hence, different approaches to estimate the mass transfer coefficient based on film theory have been proposed. However, the mass transfer coefficient across the concentration polarization layer is not one of the characteristic transport parameters in the SKK model [3]. The interplay of solute transport coupled with osmotic water fluxes holds significant importance in membrane technology. Ordered mass transfer across cell membranes plays a crucial role in various physiological processes. Artificial membranes, applied across diverse fields, including desalination, employ different types of artificial membranes [4]. The analysis of such phenomena commonly involves the use of Kedem-Katchalsky (K-K) equations and their improved versions [4]. The initial results were derived using the Spiegler-Kedem-Katchalsky model, an irreversible-thermodynamics-based approach. This modeling approach aims to determine the phenomenological parameters of mass transfer for each membrane/salt system, including salt permeability (Ps) and the mass transfer coefficient (k). In any membrane transport process, a boundary layer problem arises, leading to variations in solute concentration at the membrane-liquid interface. The mass transfer coefficient becomes a function of feed flow rate, cell geometry, and the solute system. Current recognition supports the use of a three-parameter model, such as the Spiegler-Kedem model, for a more accurate description of the transport processes occurring within RO membranes [4].

2. Theoretical and Analytical Aspects

The approach used in this work primarily relies on data collected from several RO pilot plants in the Kurdistan region of Iraq as a basis for studying the parameters affecting RO process performance. The collected data includes ranges of applied pressure, temperature, feed water type and TDS.

The calculations of the mass transfer parameters in the current work are based on a reference RO membrane (ESPA4-LD-4040), a three stages RO process, a three-year membrane age with 95% and 85% recovery. Additional conditions include permeate flow of 20 m^3/h, pH 7, a constant feed TDS of 800 mg/l, a constant feed-water pump pressure of 15 bar, and feed-water temperatures of 4, 8.2, 25, 30, and 42^oC. The Spiegler–Kedem–Katchalsky irreversible thermodynamics model is employed; it operates on a non-equilibrium basis, treating the membrane as a black box where relatively slow processes approach-equilibrium. In this context, the intricacies of the transport mechanisms and the membrane's structural details are overlooked. The model serves as a transport framework illustrating the ion transport mechanism through membrane pores within a solvent-salt system, grounded in the thermodynamics of irreversible process. Solute transport across the RO membrane is delineated by the Spiegler and Kedem-Katchalsky equations. These equations combine the transport processes of diffusion and convection for uncharged molecules, as expressed in the following two equations [4]:

$$J_w = A \times (\Delta p - \Delta \pi) \quad (1)$$

$$J_s = B \times (C_m - C_p) \quad (2)$$

Expressed as J_w and J_s, the solute flux and solvent flux, respectively, are influenced by the trans-membrane pressure (Δp) and the osmotic pressure ($\Delta \pi$), and the latter of which is typically dependent on salinity. The variables C_m and C_p represent the salt concentrations at the membrane surface and in the permeate, respectively. The parameters A and B denote the water permeability and salt permeability, respectively. The Spiegler–Kedem-Katchalsky model, rooted in irreversible thermodynamics, is employed to determine the phenomenological parameters of mass transfer for each membrane/salt system—specifically, the salt permeability (P_s) and the mass transfer coefficient (k) [3]. Reports of Zhao [5] indicate that the combined Spiegler-Kedem/film theory model is employed to provide the most accurate description of experimental data, especially when utilizing a spiral-wound polymer membrane. This particular membrane exhibits high sensitivity to feed temperature and, to a lesser extent, to the feed-flow rate [6].

The RO data were subjected to analysis using the Spiegler-Kedem-Katchalsky model to concurrently estimate membrane transport

parameters and k. It is widely acknowledged that the hydrodynamic conditions of a membrane system are influenced by factors such as flow rate, flux, recovery, feed pressure, pressure drop, transmembrane pressure drop, and temperature. Other operational considerations encompass the introduction of various chemicals, including pH control, antiscalants, or biocides. Although membrane systems may be maintained in a comparable but not identical manner, the operating conditions exert a significant impact on solute mass-transfer coefficients (MTCs). The interrelation of flow rate, flux, recovery, feed pressure, pressure drop, and transmembrane pressure drop collectively influences all aspects of solute MTCs.

The mass-transfer calculations were undertaken using a set of mathematical equations listed in Table 1.

Table 1. The mathematical equations used in mass transfer calculations

No.	Mathematical equation	Definition of the property estimated	Unit	Parameters definition	Reference
1	$SP = 100\% \times \frac{C_p}{C_f}$	SP (Salt passage)	-	C_f=salt concentration (feed) C_p= permeate conc.	[7]
2	$SR = 100\% - SP$	SR (Salt rejection)	-	SP salt passage	[7]
3	$C_c = C_f \times (1 - R(1 - SR)/(1 - R)$	C_c (TDS concentrate)	*mg/l*	R= recovery %	[7]
4	$\pi_f = C_f \times (\frac{0.8}{1000})$	π_f (Feed osmotic pressure)	*bar*	0.8/1000= rule of thumb	[7]
5	$\pi c = C_c \times (\frac{0.8}{1000})$	π_c (Permeate osmotic pressure)	*bar*	0.8/1000= rule of thumb C_c = concentration of concentrate	[7]
6	$\pi_{fc} = (\pi_f + \pi_c)/2$	π_{fc} (Average osmotic feed&conc.)	*bar*	π_f= feed osmotic pressure π_c=permeate osmotic pressure	[7]
7	$\pi_p = 0.05 \times \pi_{fc}$	π_p (Brackish water)	*bar*	π_p=0.05×π_{fc} for Brackish water	[7]
8	$\Delta\pi = \pi_{fc} - \pi_p$	$\Delta\pi_{av}$ (Difference of avg. osmotic pressure feed – conc. and osmotic pressure permeate)	*bar*	π_{fc} =Average osmotic feed&conc. π_p=0.05×π_{fc} for brackish water	[7]
9	$NDP = P_f - (\frac{\Delta P_e}{2}) - \Delta\pi_{av.} - P_p$	Net driving pressure (NDP)	*bar*	p_f= feed pressure pump Pp = 0(negligible permeate pressure) ΔP_e=0.2(suction head loss)	[7]
10	$J_w = Q_w/A_e$	(J_w) Water flux for membrane	$l/m^2\ h$	Q_w =20 m^3/h(permeate water flow rate) A_e =7.43 m^2(membrane area per element)	[7]
11	$Kw = J_w/NDP$	(K_w) Membrane permeability for water	$l/m^2\ bar.h$	NDP = net deriving pressure J_w = permeate flux	[7]
12	$C_{fc} = (C_f + C_c)/2$	(C_{fc}) Average feed-con. concentration	*mg/l*	C_f= salt concentration (feed) C_c = concentration of concentrate	[7]
13	$C_p = C_{fc} \times (1 - SR)$	(C_p) Permeate concentration	*mg/l*	C_{fc} = average feed-con. concentration SR salt rejection %	[7]
14	$J_s = Q_w/A_e$	(Js) Salt flux	$l/m^2\ h$	Q_w = 20 m^3/h(permeate water flow rate) A_e = 7.43m^2(membrane area per element)	[7]
15	$Ks = J_s \times (\frac{C_p}{C_{fc}})$	(K_s) Membrane permeability for salt	$l/m^2\ h$	Js =Salt flux C_{fc} = average feed-con. concentration C_p = permeate conc.	[7]

16	$J_w = A \times (\Delta P - \Delta\pi)$	(J_w)Water flux	$l/m^2\,h$	A= membrane permeability for water Δp = Pressure gradient Δπ = Osmotic pressure	[7]
17	$J_v = B \times (C\delta 1 - C_p)$	(J_v)Salt flux	$l/m^2\,h$	B membrane permeability for salt $c\delta 1$ conc. At membrane C_p= Permeate conc.	[7]
18	$\Delta\pi = RT(C\delta 1 - C_p)$	($c\delta 1$) Concentration at membrane Surface	bar	R=0.0802 ($l.bar/K.mol$) T=4-42℃ C_p= Permeate conc. $\Delta\pi$ =Osmotic pressure	[8]
19	$k = \frac{J_v}{\ln\{\left(\frac{\Delta p}{\Delta\pi}\right) * [1 - \left(\frac{J_v}{J_w}\right)]}$	(k) Mass transfer coefficient	m/h	Δp = Pressure gradient $\Delta\pi$ = Osmotic pressure J_w Permeate flux J_v Salt flux	[9]

3. Results and Discussion

As previously documented in the literature, temperature has the potential to modify solvent properties, including solvent viscosity and solute diffusivity. Additionally, temperature can influence the physical attributes of polymeric membranes, such as pore size and potentially the solvent diffusivity within the membrane. It's noteworthy that the effects on solvent and membrane material may not be synchronized. According to the study of Zhao [5], polymer membranes exhibit a high sensitivity to variations in feed temperature; an increase in feed temperature from 20 to 40 degrees Celsius led to a remarkable 60% rise in permeate flux. Intriguingly, a minimum flux was observed at an intermediate feed temperature, suggesting intricate physical changes within the membrane as the temperature increased. In summary, the performance of a diffusion-controlled membrane, as per a simplified solution diffusion model, is characterized by two fundamental coefficients: K_w (membrane permeability for water) and Ks (membrane permeability for salt). These coefficients are constants linked to the specific physical and chemical characteristics of each membrane. However, in reality, numerous factors can influence mass transfer coefficients (MTCs) (mass transfer coefficient). Zhao [5] demonstrated the important role of membrane-solute-solvent interactions and their impact on the solute mass transfer. He highlighted the complex and mixed effects of these interactions.

The estimated numerical values for mass transfer coefficient, water and salt permeability, water and salt fluxes, and salt rejection percentage at 95 % and 85% recovery are listed in Table 2 and Table 3, respectively.

Table 2. The estimated numerical values for the mass transfer coefficient, water and salt permeability, water and salt fluxes, and salt rejection percentage at 95% recovery

Exp.	Temperature (℃)	Permeate TDS (*mg/l*)	*Jw* *l/m².h*	*Js* *l/m².h*	K_w *l/m².bar.h*	K_s *l/m².h*	*K* *m/h*	SR%	NDP (*bar*)
1	4	150.19	3331.3	10.106	280.4	505.3	3.189	81.23	9.60
2	8.2	201.29	2948.7	13.550	270	677	4.28	74.84	9.97
3	25	365.85	2384.7	10.231	292.5	1231	3.858	54.27	9.20
4	30	402.71	1785.4	13.551	235.4	1355.1	4.227	49.66	11.43
5	42	477.95	1472	16.0818	225	1608.2	4.932	40.25	11.96

Table 3. The estimated numerical values for the mass transfer coefficient, water and salt permeability, water and salt fluxes, and salt rejection percentage at 85% recovery

Exp.	Temperature (℃)	Permeate TDS (*mg/l*)	*Jw* *l/m².h*	*Js* *l/m².h*	*Kw* *l/m².bar.h*	*Ks* *l/m².h*	*K* *m/h*	SR%	NDP (*bar*)
1	4	37.03	2275.3	2.492	212.9	124.6	0.85	95.37	12.95
2	8.2	44.36	2116.6	2.984	227.7	149.2	1.068	94.46	11.82
3	25	94.73	1293.4	6.374	210.8	318.7	2.582	88.16	12.77
4	30	118.42	1186.9	7.970	209.9	398.5	3.288	85.20	12.82
5	42	189.84	1039.5	12.775	207.4	638.8	5.302	76.27	12.98

The percent recovery is calculated by multiplying the ratio of permeate flow rate to feed flow rate by 100. The percentage of recovery is inversely related to the permeate flow rate and the percentage of rejection, assuming other factors such as feed water TDS, operating pressure, and feed water temperature remain constant. When the percentage of water recovery is low, more water is drained and lost, but the RO membrane's performance is enhanced. Manufacturers of RO systems typically propose a recovery rate to balance performance and economics [10]. In Fig. 1, salt rejection (%) for 95% recovery at a temperature of 4°C is 81.23% while for 85% recovery it is 95.37. For the maximum temperature which is 42°C, at recovery 95% and 85% the value are 40.26 % and 76.27% respectively. This means that increasing the feed temperature from 4 to 42°C resulted in a decrease in salt rejection (%) by 50.45% for 95% recovery and 20.02% for 85% recovery. Apart from the solution viscosity decrease, there is an increase in salt diffusivity. This situation may contribute to decreasing membrane fouling. The same trend was pointed out by Farhat et al. [11] who declared that when temperature increased from 24°C to 56°C, salt rejection decreased from 80% to 68%.

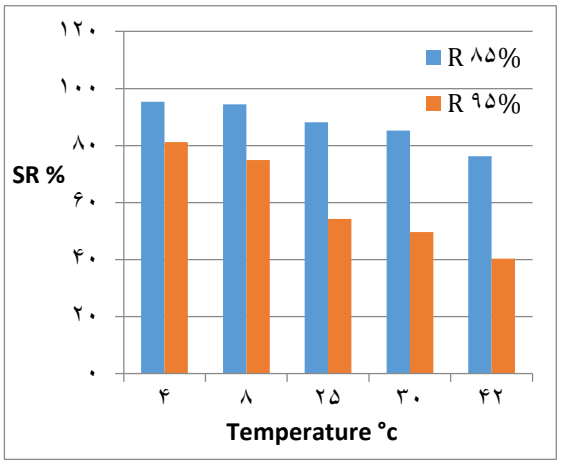

Fig. 1. Salt rejection(%) versus temperature at a constant pressure of 15 bar and 800 *mg/l* TDS of feed water

Boussouga and Lhassani [12] indicated that salt permeability P_s is contingent upon the effective charge of the membrane, as well as the nature and concentration of the solute. Meanwhile, the mass-transfer coefficient (k) is influenced by the physico-chemical properties of the solution and the hydrodynamic conditions within the system. As shown in Figs. 2 and 3, when temperature increases, the coefficients (k, k_s) for both investigated recoveries, 95% and 85%, increase from (3.188 *m/h*, 505.3 l/m^2h) at 4*℃* for 95% recovery to (4.93 *m/h*, 1472 l/m^2h) at 42*℃*, respectively. Also, for 85% recovery, they were (0.85 *m/h*, 124.6 l/m^2h) at a temperature 4*℃* and similarly increased to (5.302 *m/h*, 638.8 l/m^2h) at 42*℃*. However, the result showed that the mass-transfer coefficient and salt permeability increased by 35.34% and 68.57% for 95% recovery, and 83.97% and 80.50% for 85% recovery. Wang et al. [13] anticipated that phenomenological parameters, specifically water permeability and salt permeability, are frequently employed to assess membrane performance in RO. Traditionally, these parameters are assumed to remain constant and independent of each other. However, recent experimental studies suggest a potential variation in salt permeability based on feed salt concentration. The observed increase in permeate salt concentration and water flux surpasses the rise in salt concentration difference across the membrane, leading to an augmented salt permeability with increasing hydraulic pressure. This influence of hydraulic pressure on salt permeability becomes more pronounced at higher feed concentrations, attributed to the heightened partitioning of ions into the membrane, consequently enhancing salt flux through both advection and diffusion.

Moreover, Hung et al. [8] noted that the osmotic pressure of a salt solution increases as the temperature rises. Depending on the fluctuation in the water diffusion coefficient, the water permeability coefficient may be raised or lowered. As predicted in the current work (K_w) for both investigated recoveries, 95% and 85%, (as shown in Fig. 4), (K_w) was 280.4 $l/m^2bar.h$ at temperature 4*℃* for 95% recovery, and it was 225 $l/m^2bar.h$ at 42*℃*, respectively. Also, for 85% recovery, it was 212.9 $l/m^2bar.h$ at temperature 4*℃* and 207.4 $l/m^2bar.h$ for 42*℃*, respectively. Therefore, the permeate flux (Jw) may rise or decrease depending on which factor has the most significant effect. Water flux decreased by 55.81% for 95% recovery and 54.31% for 85% recovery, and K_w decreased by 19.75% for 95% recovery and by 2.58% for 85% recovery. The investigation by Okamoto and Lienhard [14] demonstrated that as membrane water permeability rises, the feed pump pressure asymptotically decreases to the osmotic pressure of the brine. In the context of SWRO, elevating membrane water permeability from (1) to (3) *l m h/bar* correlates with a reduction in feed pump pressure from 70 to 63 *bar*. In contrast, according to Wang et al. [13], water permeability remains consistent even when salt concentration and hydraulic pressure undergo extensive variations. This stability is attributed to the prevailing influence of friction between water and the membrane in determining the hydraulic pressure drop across the membrane. This friction factor is unaffected by salt concentration and hydraulic pressure,

resulting in a constant water permeability irrespective of the operational conditions.

It is worthy to note that the salt flux also increases when the temperature increases, by 59.13% for 95% recovery and 80.50% for 85% recovery. Figure 5 shows that salt flux increases from 10.2 l/m^2h at 4℃ to 16.818 l/m^2h at 42℃ for 95% recovery. The same observations are noted for 85% recovery, where salt flux increases from 2.492 l/m^2h at 4℃ to 12.8 l/m^2h at 42℃.

The permeate flux (J_w) may rise or decrease depending on which factor has the most significant effect; water flux decreased by 55.81% for 95% recovery and 53.19% for 85% recovery. Figure 6 shows that permeate flow decreases at both recoveries, 95% and 85%, from 3331.3 l/m^2h at 4℃ to 1472 l/m^2h at 42℃ and 2275.3 l/m^2h at 4℃ to 1039.5 l/m^2h at 42℃, respectively. Thus, water flux decreased by 55.81% for 95% recovery and 54.31% for 85% recovery.

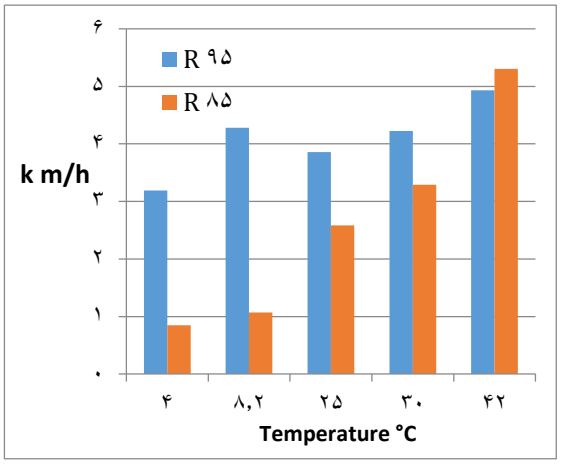

Fig. 2. Mass transfer coefficient versus different temperature at a constant pressure of 15 bar and 800 mg/l TDS of feed water

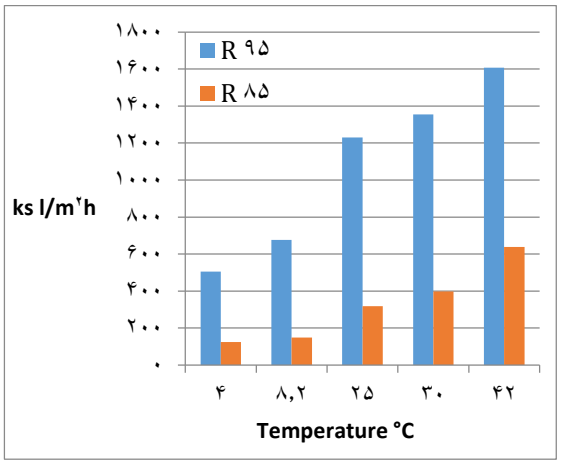

Fig. 3. Salt permeability versus temperature at constant pressure of 15 bar and 800 mg/l TDS of feed water

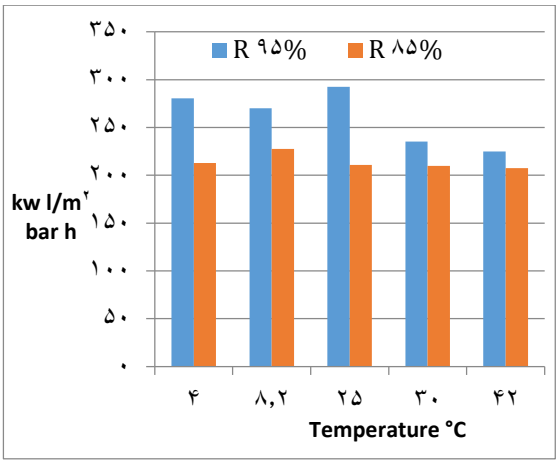

Fig. 4. Water permeability versus temperature at a constant pressure of 15 *bar* and 800 *mg/l* TDS of feed water

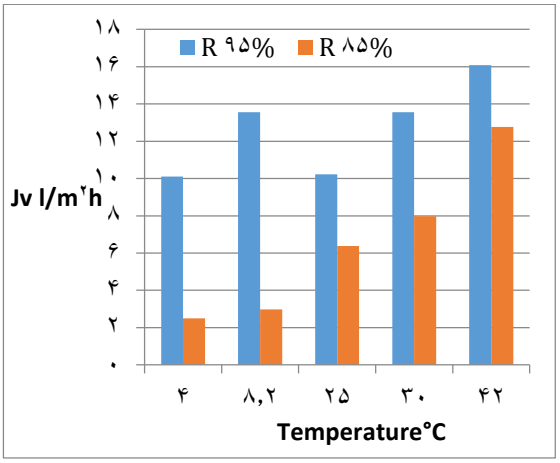

Fig. 5. Salt flux versus temperature at a constant pressure of 15 *bar* and 800 *mg/l* TDS of feed water

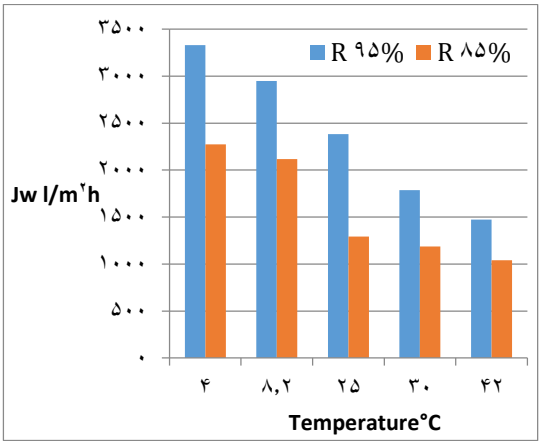

Fig. 6. Permeate flux versus different temperature at a constant pressure of 15 *bar* and 800 *mg/l* TDS of feed water

It was reported that for constant product flow, when the temperature of feed water increases, the product water salinity increases, and the required applied pressure decreases; therefore, energy consumption decreases [15].

The productivity increases when the RO unit operates at high temperature. Fewer membrane elements will be required if the permeate flow is allowed to increase as the temperature increases; this situation results in a remarkable saving in the cost of water production.

However, as shown in Fig. 6, permeate flow decreases at both recoveries, 95% and 85%, from 3331.3 *l/m²h* at 4℃ to 1472 *l/m²h* at 42℃, and 2275.3 *l/m²h* at 4℃ to 1039.5 *l/m²h* at 42℃, respectively. The reason may be the application of constant feed pressure, which indicates that the increase in temperature of feed water had a reverse effect on permeate flow. Hung et al. [8] reported that *Δp* of the feed solution affects positively the permeate flux. In the current work, *Δp* decreases by 51.32% for 85% and by 45.16% for 95% recovery, causing a decrease in permeate flux by 54.31% for 85% recovery and by 55.81% for 95% recovery.

The reason can be demonstrated by the fact that the permeate flux is directly proportional to the net driving force (*Δp-Δπ*). The pace of recovery influences salt passage and product flow. As the recovery rate increases, so does the salt concentration on the feed-brine side of the membrane, resulting in a greater salt flow rate across the membrane. In addition, a higher salt concentration in the feed-brine solution raises the osmotic pressure, hence decreasing the NDP and the product water flow rate.

In any RO system, the maximum achievable recovery is typically dictated not only by the limiting osmotic pressure but also by the concentration of salt in the feed water and its propensity to precipitate on the membrane surface. As depicted in Figs. 7 and 8, when the permeate flux was 3331.3 *l/m²h* at 9.6 *bar*, it exhibited a decrease to 1472 *l/m²h* at 11.96 *bar*. Similarly, it decreased from 2275.3 l/m²h at 12.65 *bar* to 1039.5 *l/m²h* at 12.98 *bar* for both 95% and 85% recovery, respectively.

The negative deviation in the plot of permeate flux vs. net driving pressure may be attributed to the non-linearity of the pressure drop in the permeate channel spacer with the permeate flow rate, as noted in previous studies [10], [16].

In this connection, the results shown in Figs. 9 and 10 revealed that an increase in feed water salinity causes a reduction in the permeate flow rate and salt rejection, and an increase in the permeate salinity.

The TDS of permeate water increases for both recoveries, 95% and 85%, and this result in a reduction in salt-rejection percentage and permeate flux: at 95% recovery from 3331.3 *l/m²h* at 81.23% salt rejection to 1472 *l/m²h* at 40.26% salt rejection, and from 2275.3 *l/m²h* at 95.37% salt rejection to 1039.5 *l/m²h* at 76.27% salt rejection for 85% recovery. It was declared that when TSD of permeate increases salt rejection will decreases due to temperature increase and this leads to a decrease in permeate flow [11].

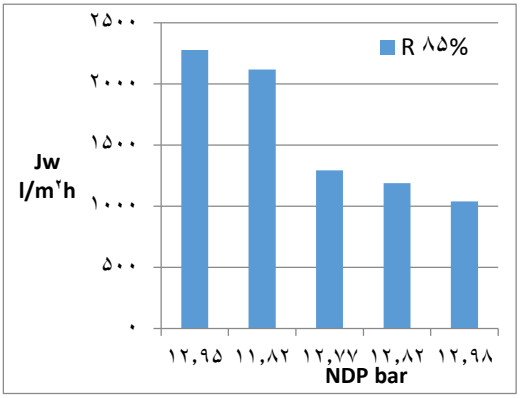

Fig. 7. Permeate flux versus NDP at a constant pressure of 15 bar and 800 mg/l TDS of feed water for 85% recovery

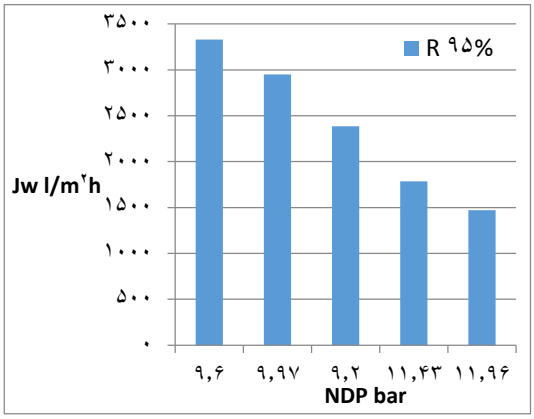

Fig. 8. Permeate flux versus NDP at a constant pressure of 15 bar and 800 mg/l TDS of feed water for 95% recovery

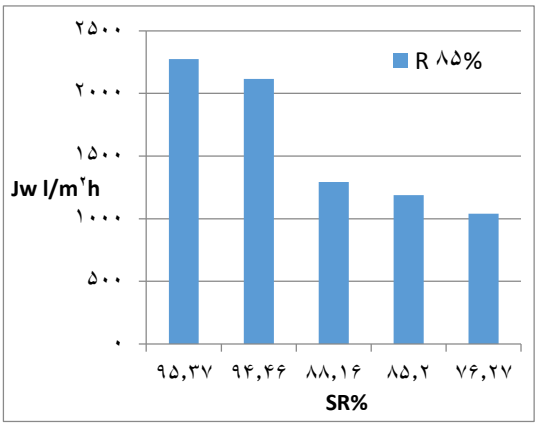

Fig. 9. Permeate flux versus SR% at a constant pressure of 15 *bar* and 800 *mg/l* TDS of feed water at for 85% recovery

The modeling studies revealed a high sensitivity of the mass transfer coefficient to

variations in feed salt concentration and temperature; specifically, the mass transfer coefficient (k) and membrane permeability (PM) exhibit a decline with an increase in feed salt concentration and a decrease in feed temperature [5]. When temperature increases from 4℃ to 42℃, the mass transfer coefficient increases, and membrane permeability for salt increases by 83.97% and 80.50% for 85% recovery, respectively, while water permeability decreases by 2.58% for 85% recovery from 4℃ to 42℃ because of increasing TDS of permeate and the operation at constant pressure for all temperatures. It was also interesting that a general empirical model for the investigated RO system was developed. The model was estimated with a relatively high R^2 of 0.94. The model describes the correlation between the mass transfer coefficient and feed-water temperature, water and salt permeability at 85% recovery (See Figs. 11 and 12). The model is represented by the following equation:

$$k = (1.1124 \times x) - 0.7192 \quad (3)$$

where k is the mass transfer coefficient, x is the feed-water temperature, water permeability, and salt permeability.

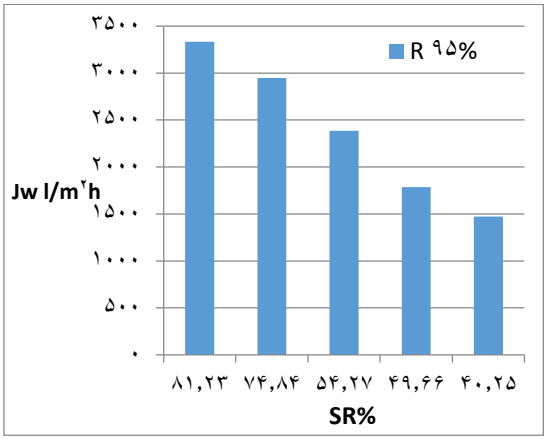

Fig. 10. Permeate flux versus SR% at a constant pressure 15 *bar* and 800 *mg/l* TDS of feed water at for 95% recovery

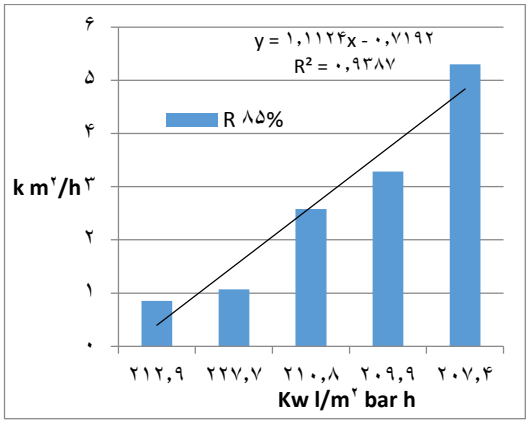

Fig. 11. Variation of mass transfer coefficient with water permeability at different temperature for 85% recovery

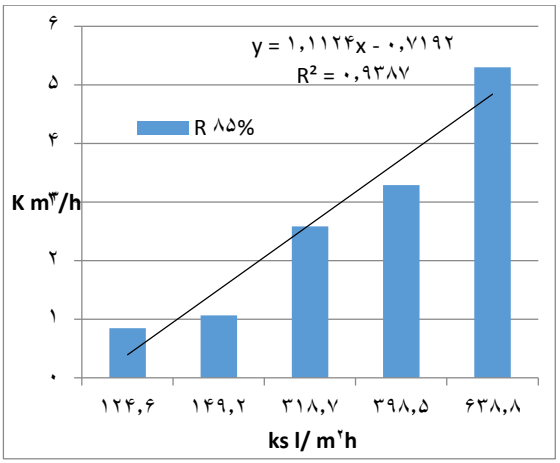

Fig. 12. Variation of mass transfer coefficient with salt permeability at different temperature for 85% recovery

4. Conclusions

The Spiegler-Kedem-Katchalsky model stands as a powerful tool employed to ascertain phenomenological parameters of mass transfer within RO membrane systems. This includes determining the mass transfer coefficient and membrane permeability for salts, considering variables such as temperature and % recovery. Furthermore, it proves valuable in the formulation of mathematical models that articulate the relationships between the mass transfer coefficient and feed-water temperature, water permeability, and salt permeability. The development of solute mass transfer models is of paramount importance for the ongoing evaluation of membrane performance and the identification and correlation of phenomenological parameters within the membrane system. This model can also aid in estimating the sensitivity of permeate water quality to variations in temperature and % recovery, as well as in assessing permeate water quality and determining membrane cleaning frequency.

Funding Statement

This research did not receive any specific grant from funding agencies in the public, commercial, or not-for-profit sectors.

Conflicts of Interest

The author declares that there is no conflict of interest regarding the publication of this article.

Authors Contribution Statement

Dnya Sharif Mohammed: Conceptualization, Methodology, Literature Review, Data Analysis, Investigation, Writing – Original Draft

Preparation, Writing – Review & Editing, Visualization, Project Administration.

Ibtisam Kamal: Conceptualization, Supervision, Methodology, Validation, Writing – Review & Editing, Scientific Guidance.

Abdulsamad Abdulhameed: Data Curation, Resources, Investigation, Validation, Technical Support through the Provision of Field and Operational Data.

References

[1] Hailemariam, R. H., Woo, Y. C., Damtie, M. M., Kim, B. C., Park, K. D. and Choi, J. S., 2020. Reverse osmosis membrane fabrication and modification technologies and future trends: A review. *Advances in Colloid and Interface Science*, 276, p. 102100. doi: 10.1016/j.cis.2019.102100.

[2] Murthy, Z. V. P. and Gupta, S. K., 1997. Estimation of mass transfer coefficient using a combined nonlinear membrane transport and film theory model. *Desalination*, 109(1), pp. 39–49. doi: 10.1016/S0011-9164(97)00051-9.

[3] Wang, L., He, J., Heiranian, M., Fan, H., Song, L., Li, Y. and Elimelech, M., 2023. Water transport in reverse osmosis membranes is governed by pore flow, not a solution-diffusion mechanism. *Science Advances*, 9(15), pp. 1–12. doi: 10.1126/sciadv.adf8488.

[4] Spiegler, K. S. and Kedem, O., 1966. Thermodynamics of hyperfiltration (reverse osmosis): Criteria for efficient membranes. *Desalination*, 1, pp. 311–326.

[5] Zhao, Y., 2004. Modeling of membrane solute mass transfer in NF/RO membrane systems. Doctoral Dissertation, University of Central Florida, pp. 2004–2019.

[6] Goosen, M. F. A., Sablani, S. S., Al-Maskari, S. S., Al-Belushi, R. H. and Wilf, M., 2002. Effect of feed temperature on permeate flux and mass transfer coefficient in spiral-wound reverse osmosis systems. *Desalination*, 144(1–3), pp. 367–372. doi: 10.1016/S0011-9164(02)00345-4.

[7] Salinas-Rodríguez, S. G., Schippers, J. C., Amy, G. L., Kim, I. S. and Kennedy, M. D., 2021. Seawater Reverse Osmosis Desalination: Assessment and Pre-treatment of Fouling and Scaling. IWA Publishing, doi: 10.2166/9781780409863.

[8] Hung, L. Y., Lue, S. J. and You, J. H., 2011. Mass-transfer modeling of reverse-osmosis performance on 0.5-2% salty water. *Desalination*, 265(1–3), pp. 67–73. doi: 10.1016/j.desal.2010.07.033.

[9] Sutzkover, I., Hasson, D. and Semiat, R., 2000. Simple technique for measuring the concentration polarization level in a reverse osmosis system. *Desalination*, 131(1–3), pp. 117–127. doi: 10.1016/S0011-9164(00)90012-2.

[10] Al-Mutaz, I. S. and Al-Ghunaimi, M. A. Performance of reverse osmosis units at high temperatures. https://ida.memberclicks.net/assets/docs/1099.1.pdf

[11] Farhat, A., Ahmad, F., Hilal, N. and Arafat, H. A., 2013. Boron removal in new generation reverse osmosis (RO) membranes using two-pass RO without pH adjustment. *Desalination*, 310, pp. 50–59. doi: 10.1016/j.desal.2012.10.003.

[12] Boussouga, Y. A. and Lhassani, A., 2017. Study of mass transfer mechanisms for reverse osmosis and nanofiltration membranes intended for desalination. *Journal of Materials and Environmental Science*, 8(3), pp. 1128–1138.

[13] Wang, L., Cao, T., Dykstra, J. E., Porada, S., Biesheuvel, P. M. and Elimelech, M., 2021. Salt and water transport in reverse osmosis membranes: Beyond the solution-diffusion model. *Environmental Science & Technology*, 55(24), pp. 16665–16675. doi: 10.1021/acs.est.1c05649.

[14] Okamoto, Y. and Lienhard, J. H., 2019. How RO membrane permeability and other performance factors affect process cost and energy use: A review. *Desalination*, 470, pp. 0–30. doi: 10.1016/j.desal.2019.07.004.

[15] Martin-Pascual, J., Rodríguez, F. A., Reboleiro-Rivas, P., González-Lopez, J., Hontoria, E. and Poyatos, J. M., 2012. Influence of the temperature in the permeate flux of the membrane in a membrane bioreactor with moving bed biofilm reactor. *Procedia Engineering*, 44, pp. 275–277. doi: 10.1016/j.proeng.2012.08.385.

[16] Eriksson, P., 1988. Water and salt transport through two types of polyamide composite membranes. *Journal of Membrane Science*, 36, pp. 297–313. doi: 10.1016/0376-7388(88)80024-3.